Virus Research 223 (2016) 20–27

Virus Research

journal homepage: www.elsevier.com/locate/virusres

VP3 is crucial for the stability of Nora virus virions

Sajna Anand Sadanandan[a], Jens-Ola Ekström[a,c], Venkateswara Rao Jonna[b], Anders Hofer[b], Dan Hultmark[a,c,*]

[a] Department of Molecular Biology, Umeå University, SE-901 87 Umeå, Sweden
[b] Department of Medical Biochemistry and Biophysics, Umeå University, SE-901 87 Umeå, Sweden
[c] Institute of Biomedical Technology, University of Tampere, FI-33520 Tampere, Finland

ARTICLE INFO

Article history:
Received 15 March 2016
Received in revised form 15 June 2016
Accepted 17 June 2016
Available online 18 June 2016

Keywords:
RNA viruses
Nora virus
Capsid stability
Virus biology

ABSTRACT

Nora virus is an enteric virus that causes persistent, non-pathological infection in *Drosophila melanogaster*. It replicates in the fly gut and is transmitted via the fecal-oral route. Nora virus has a single-stranded positive-sense RNA genome, which is translated in four open reading frames. Reading frame three encodes the VP3 protein, the structure and function of which we have investigated in this work. We have shown that VP3 is a trimer that has an α-helical secondary structure, with a functionally important coiled-coil domain. In order to identify the role of VP3 in the Nora virus life cycle, we constructed VP3-mutants using the cDNA clone of the virus. Our results show that VP3 does not have a role in the actual assembly of the virus particles, but virions that lack VP3 or harbor VP3 with a disrupted coiled coil domain are incapable of transmission via the fecal-oral route. Removing the region downstream of the putative coiled coil appears to have an effect on the fitness of the virus but does not hamper its replication or transmission. We also found that the VP3 protein and particularly the coiled coil domain are crucial for the stability of Nora virus virions when exposed to heat or proteases. Hence, we propose that VP3 is imperative to Nora virus virions as it confers stability to the viral capsid.

1. Introduction

Nora virus is a small RNA virus that causes persistent, non-pathological infection in *Drosophila melanogaster* (Habayeb et al., 2006). It is an enteric virus that is transmitted via the fecal-oral route and high virus titers have been observed in the feces of infected animals (Habayeb et al., 2009). It possibly defines a new family of picorna-like viruses. Based on sequence comparisons of the replicative enzymes, the Nora virus is most closely related to viruses of the families *Picornaviridae*, which infect vertebrates, and *Iflaviridae*, which infect insects (Habayeb et al., 2006; Koonin et al., 2008). Yet, the Nora virus has a unique size and organization of its genome. *Picornaviridae* includes important human enteroviruses such as the polio virus, while honeybee pathogens like the deformed wing and sacbrood viruses belong to *Iflaviridae*. Some members of these families are able to establish persistent infections in their hosts, probably contributing to problems such as the post-polio syndrome in humans and the colony collapse disorder in honeybees (Prisco et al., 2011; Baj et al., 2015). The Nora virus may be a useful model to study the phenomenon of RNA virus persistence. For that purpose, we found it important to characterize the virus in more detail.

Nora virus has a 12333 nucleotides long (Ekström et al., 2011) single-stranded RNA genome of positive polarity (Habayeb et al., 2006). Experimental work and sequence analysis have indicated that, out of the four open reading frames in the Nora virus genome, ORF1 encodes an inhibitor of the RNAi defense mechanism (van Mierlo et al., 2012), while ORF2 encodes a long polyprotein with the helicase, protease and polymerase regions that are closely related to the corresponding proteins found in the replicative cassettes of picorna-like viruses (Habayeb et al., 2006; Koonin et al., 2008). No sequence similarity was detected between ORF4 and other known virus products, but experimental evidence has shown that it encodes a polyprotein that is cleaved into three capsid proteins, VP4A, B and C (Ekström et al., 2011). However, the ORF3-encoded protein, VP3, remains largely uncharacterized.

Small amounts of an ORF3-encoded protein, with an estimated molecular mass of 35 kDa, were detected in the virions during mass spectrometry analysis of the VP4 capsid proteins (Ekström et al., 2011). This suggested that the VP3 protein was associated with the structural proteins. The first 71 nucleotides of ORF3 overlap with

* Corresponding author at: Department of Molecular Biology, Umeå University, SE-901 87 Umeå, Sweden.
E-mail address: dan.hultmark@umu.se (D. Hultmark).

http://dx.doi.org/10.1016/j.virusres.2016.06.011

the C-terminus of ORF2 and therefore, translation of ORF3 is likely to occur with a frame shift mechanism. The resulting VP3 protein is 281–304 amino acids long, depending on the exact position of the frame shift, and the predicted molecular mass approximately 31–34 kDa. Based on the sequence, Ekström et al. (2011) predicted an α-helical secondary structure for the N-terminal 200 amino acids of VP3, and that this part of the protein is likely to form a coiled-coil domain. However, experimental evidence is still lacking for this model. Thus far, the role of VP3 in the life cycle of Nora virus has not been investigated.

We have now used the cDNA clone of Nora virus (Ekström et al., 2011) to study the importance of VP3 in virion assembly and structural stability, by generating VP3 mutants. During the course of this study, we observed that VP3 was important for the transmission of Nora virus via the fecal-oral route. Consequently, we hypothesized that the presumed coiled-coil domain in this protein was important for the stability of the virus particles. To address this hypothesis, we compared the stability of wild-type virions to that of VP3 mutant virions. We found that mutant virions lacking VP3 or harboring a disruption in the predicted coiled coil domain were labile under heat and protease treatments, while the wild type virions survived these conditions.

2. Materials and methods

2.1. Cloning, expression and purification of Nora virus VP3

Nora virus ORF3 was cloned into the multiple cloning site of the pETM-MBP1a expression vector (Pryor and Leiting, 1997) using forward (GCTTCCATGGCATTAAAAGAGGAGATTTTTGATCAA) and reverse (GCTTGGTACCTTACATAGAGTCATAAATTACTGATGTGCT) primers. The pETM-MBP1a vector contains a hexa-Histidine tag followed by the maltose binding protein (MBP) and a *Tobacco etch virus* (TEV) cleavage site, after which the ORF3 sequence was inserted. This construct was transformed into Rosetta (DE3) cells (Fu et al., 2007), which were then grown overnight in an auto-induction LB medium (Edwin et al., 2014) at 20 °C. Since it is tagged with the maltose binding protein, the expressed VP3 protein could be isolated using an amylose resin affinity matrix (NEB), according to the instructions provided by the manufacturer. The isolated protein was cleaved from its MBP tag using the TEV protease and thereafter purified by NiNTA agarose chromatography (Qiagen) in order to remove both MBP and TEV protease. The now-untagged VP3 protein was subjected Q-Sepharose (GE healthcare) chromatography in order to obtain pure VP3 (Fig. 1A, lane 2).

2.2. Analysis of VP3 oligomers by GEMMA

Purified Nora virus VP3 protein was dissolved in 20 mM ammonium acetate pH 7.8 to a final concentration of 0.05 mg/ml. GEMMA analysis was performed as described in Rofougaran et al. (2008).

2.3. Analysis of VP3 oligomers by cross-linking

For cross-linking, purified VP3 (0.25 mg/ml, final concentration) was treated with dimethyl pimelimidate (Sigma, 0.75 mg/ml, final concentration), both dissolved in phosphate buffered saline, pH 8.0. The reaction was incubated at room temperature for 30 min, and thereafter stopped by addition of Tris-HCL buffer, pH 8.0, to a final concentration of 20 mM. Both native and cross-linked VP3 were treated with 2× Laemmli protein sample buffer (100 mM Tris pH 6.8, 2% SDS, 0.001% bromophenol blue, 20% Glycerol and 2% β-mercaptoethanol) at a 1:1 ratio, heated at 95 °C for 10 min, and then run on a 13.6% SDS-polyacrylamide gel (29:1 acrylamide/bis-acrylamide) as described (Laemmli, 1970).

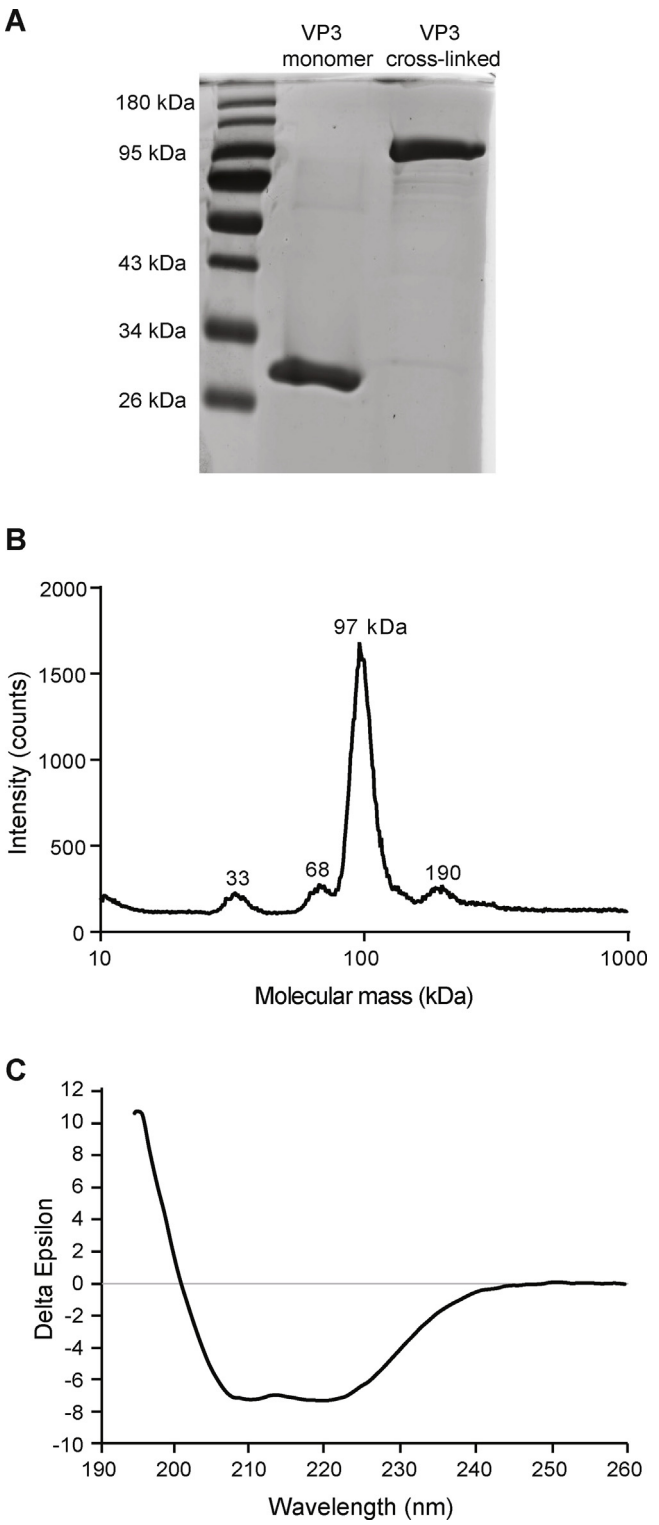

Fig. 1. Structural Characterization of Nora virus VP3 (A) SDS-polyacrylamide gel electrophoresis of VP3 monomer and cross-linked VP3 trimer. Marker: PageRuler prestained protein ladder (Thermo Scientific). (B) Nano-Electrospray GEMMA analysis of Nora virus VP3 (0.05 mg/ml) at 2 psi capillary pressure. (C) Far-UV Circular dichroism analysis of Nora virus VP3, presented as an average of 5 scans taken at 50 nm/min, showing a spectrum that is typical for α-helical proteins.

2.4. Circular dichroism

CD spectra of Nora virus VP3 were obtained on a Jasco Spectropolarimeter model J-715 (Jasco Corporation). The spectra were collected at 25 °C in a standard phosphate buffered saline (pH 7.4) using a quartz cuvette of 0.1 cm path length. Shown spectra represent the average of five scans at a speed of 50 nm/min. Only the far UV region from 190 nm to 260 nm was analyzed.

2.5. Sequence data and secondary structure prediction

Secondary structures were predicted using the NetSurfP 1.1 server (Petersen et al., 2009) and the NetTurnP 1.0 server (Petersen et al., 2010), accessed via the CBS Prediction Servers (http://www.cbs.dtu.dk/services). Prediction for coiled coil was performed using the Marcoil server (Delorenzi and Speed, 2002) accessed via the Bioinformatics Toolkit at the Max-Planck Institute for Developmental Biology (http://toolkit.tuebingen.mpg.de/marcoil), the Paircoil2 server (McDonnell et al., 2006) and the MultiCoil server (Wolf et al., 1997), both accessed at the MIT Computer Science and Artificial Intelligence Laboratory (http://groups.csail.mit.edu/paircoil2.html and http://groups.csail.mit.edu/cb/multicoil/cgi-bin/multicoil.cgi)

2.6. Establishing wild type and mutant Nora virus infection in flies

The infectious cDNA clone of Nora virus (Ekström et al., 2011) was used to construct VP3 mutants using standard molecular cloning techniques. List of primers used to construct the different mutants is given in Table S1 of Supplementary materials. All experiments were performed using *Relish*^{E23} (Hedengren et al., 1999) flies, reared at 25 °C on standard mashed-potato fly food (Yang et al., 2015). The constructed clones were microinjected into dechorionated syncytial-stage embryos (Spradling, 1986). To induce expression the larvae were subsequently reared on fly food containing 0.5 mM $CuSO_4$, until they reached the adult stage.

2.7. Virus particle purification

Virus particles were purified from whole fly extract and from the feces of infected flies. To extract virus particles from infected flies, 10–15 flies were homogenized with a homogenizing pestle in NT-buffer (100 mM NaCl and 10 mM Tris-HCl, pH 7.4). To extract virus particles from feces, feces was collected from 10 to 15 flies by keeping them in 15-ml centrifuge tubes for 2–4 h and washing the tube walls with NT-buffer. Triton X-100 was added to a final concentration of 0.5% to the whole fly extract and 0.01% to the feces. Virus purification was performed as described previously by Anderson et al. (1966). Briefly, the virus particles were pelleted by centrifugation at 38000 rpm for 70 min using the SW41Ti rotor (Beckman Coulter). Pelleted particles were dissolved in 1 ml NT-T buffer (NT buffer, 0.01% Triton X-100) and loaded on top of the sucrose gradients. Rate-zonal separation was performed on a 35–12% (w/v) linear sucrose gradient in NT-T buffer at 38000 rpm, for 90 min in 4 °C. Gradient fractions were collected by puncturing the bottom of the tubes and collecting 0.5 ml/fraction. Quantitative RT-PCR was used to determine virus peak fractions.

2.8. Quantitative RT-PCR

Total RNA was extracted from the samples using Aurum Total RNA Mini Kit (BioRad). Quantitative RT-PCR was performed as described previously (Habayeb et al., 2009; Ekström et al., 2011) using forward primer: 5′-TTTCACTTTACTGTTGGTCTCC-3′, reverse Primer: 5′-ATTCCATTTGTGACTGATTTTATTTC-3′ and Taqman probe: 5′-FAM-AGAGTTAGTGGACAAGTTAGAGACTGGCAT-TAMRA-3′.

2.9. Protease cleavage analysis

Wild-type and mutant virus particles purified by rate-zonal separation, were subjected to protease cleavage. They were treated with, either 2000 U/ml trypsin (#T8003, Sigma-Aldrich) or 0.05 U/ml pancreatic protease (#P4630, Sigma-Aldrich), for 2 h at 37 °C. Both trypsin and protease were dissolved in phosphate saline buffer, pH 7.4. Following this, the treated particles were incubated with a protease inhibitor cocktail (#1697498, Sigma-Aldrich) and RNase A (Thermo Scientific), for 30 min at 37 °C. Total RNA was extracted and virus titer was determined by quantitative RT-PCR (as described in Section 2.6).

3. Results

3.1. VP3 forms trimers

In order to characterize VP3 biochemically, we cloned and expressed the protein in a bacterial expression vector. The purified VP3 protein runs like a 29–31 kDa protein on an SDS gel (Fig. 1A). This is in agreement with the molecular mass predicted from the sequence, 31–34 kDa, depending on the position of the amino terminus. It is also consistent with the previously estimated 35 kDa of VP3 from intact virions (Ekström et al., 2011).

Nano-Electrospray GEMMA detects the electrophoretic mobility of particles in air, which is used to calculate molecular diameter and consequently, the molecular mass of the particles. We have used this method to find the native oligomeric nature of purified VP3 protein. GEMMA shows a strong peak at 97 kDa (Fig. 1B), which corresponds with the trimeric form of VP3. Minor peaks are observed at 33, 68, and 190 kDa, suggesting the presence of minimal amounts of intermediary monomeric, dimeric and hexameric forms of the protein. As an independent test of the results obtained through GEMMA, we cross-linked VP3 using dimethyl pimelimidate and analyzed the cross-linked protein on an SDS-polyacrylamide gel (Fig. 1A). The cross-linked protein appears to be around 97 kDa, which would correspond to a VP3 trimer. Taken together, our results show that Nora virus VP3 has a propensity to form trimers.

3.2. VP3 is predominantly α-helical

Secondary structure prediction of VP3 had indicated that the N-terminal region is α-helical and that the region downstream of this showed greater likelihood for forming β-strands (Ekström et al., 2011). Circular dichroism was performed on purified VP3 to experimentally validate the predicted secondary structure. The CD spectrum of VP3 (Fig. 1C) shows a positive band at 195 nm and two negative bands at 209 nm and 220 nm. Such a spectrum is characteristic of α-helical proteins (Greenfield, 2006). On calculating the percentages of different structural elements in the protein, using the CDNN CD deconvolution software (Böhm et al., 1992), it was found to be approximately 77% α-helical, 10% β-turn, 8% random coil and the remaining antiparallel/parallel sheets. These results parallel the secondary structure prediction of Nora virus VP3 performed previously by Ekström et al. (2011)

3.3. A trimeric coiled-coil structure is predicted for VP3 homologs in Nora-like viruses

The similarity of Nora virus to previously described viruses is largely restricted to the replicative cassette encoded by ORF2, which shows homology to picorna-like viruses (Habayeb et al.,

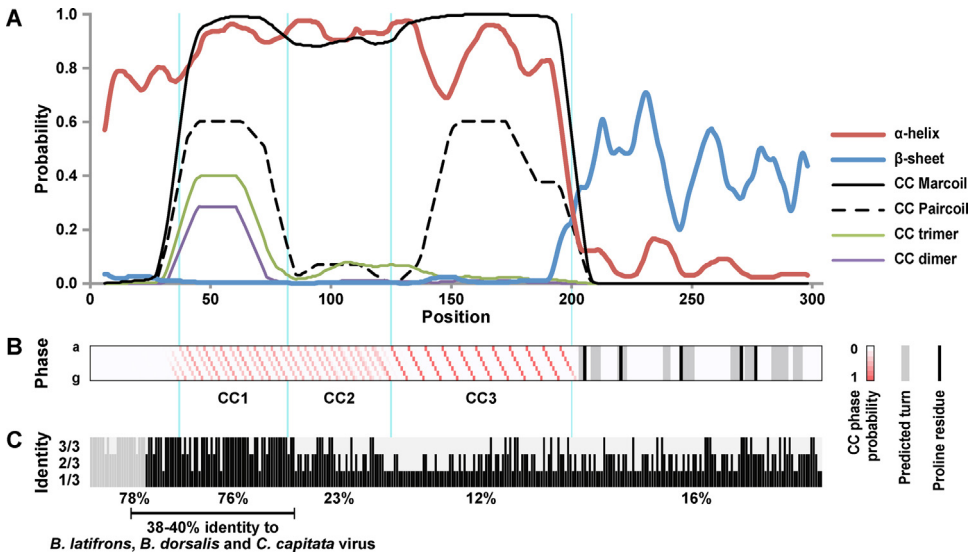

Fig. 2. Sequence analysis and secondary structure prediction of VP3. (A) Probabilities for α-helix (red), β-strand (blue) and coiled coil according to Marcoil (solid black) or Paircoil2 (dashed black), and relative probabilities for coiled coil dimers (purple) or trimers (green) are shown as sliding averages of 13 amino acids. (B) Schematic representation of predicted structural elements in VP3. The probability for each amino acid to reside in any of the seven possible positions, a-g, of a coiled coil is indicated by different shades of red. Predicted β-turns are shown in grey and helix-breaking proline residues are black. The predicted coiled coil segments, CC1-CC3, are delineated by blue lines. (C) Sequence conservation between three *Drosophila* Nora viruses, *D. melanogaster*, *D. immigrans* and *D. subobscura*; 3/3 indicates full identity. The region that overlaps with ORF2 is shown grey. The percent of residues that are fully conserved is indicated for the different sub-regions below the graph. Also shown is the region that is conserved in viruses from the tephritid flies.

2006; Koonin et al., 2008). TBLASTN search in the EST database had earlier identified ORF3- and ORF4-related EST sequences from the parasitoid wasp, *Nasonia vitripennis* (Oliveira et al., 2010; Ekström et al., 2011), showing that this wasp, or possibly its host, harbored a virus that is related to the *Drosophila* Nora virus. Secondary structure estimation showed that the VP3 homolog in this *Nasonia* Nora virus also had a putative coiled coil domain in the N-terminal part of the protein (Ekström et al., 2011). Additional Nora-like sequences are now available, allowing a more detailed comparative study of VP3-related sequences. Three novel Nora-like viruses have recently been described, two from the *Drosophila* species *D. immigrans* and *D. subobscura* and one from the moth *Spodoptera exigua* (Jakubowska et al., 2014; van Mierlo et al., 2014). Furthermore, through TBLASTN searches in the Transcriptome Shotgun Assembly database, we could retrieve additional Nora-like virus sequence assemblies from three tephritid flies, two additional moths, one ant and one parasitoid wasp (Table S2), as well as shorter sequence fragments from several other insect species. These sequences were defined as Nora-like by two criteria: a) they encode ORF4 capsid proteins of the unique Nora virus type and b) their replication cassettes are more closely related to the *D. melanogaster* Nora virus ORF2 proteins than to other picorna-like homologs. We will here refer to all Nora virus homologs as Nora viruses. Noticeably, the relationship between the different Nora viruses closely mirrors that of their insect hosts, suggesting a long history of co-evolution. ORF1 and ORF3 sequences were poorly conserved between the different Nora viruses, but an ORF3 homolog could always be identified as a separate open reading frame between the better conserved ORF2 and ORF4-related sequences.

Fig. 2 illustrates predicted secondary structure elements in the VP3 protein of *D. melanogaster* Nora virus. A region spanning the first approximately 200 amino acids displays a high probability for an α-helical conformation (red curve in Fig. 2A), with a high probability for coiled-coil formation between residues 36–200 (black curve), while the region downstream is predicted to have stretches of β-strands (blue curve) interrupted by β-turns (grey-shaded in Fig. 2B). This prediction of a secondary structure is remarkably conserved among the Nora viruses, in particular for the dipteran and lepidopteran viruses (Fig. S1). However, the primary amino acid sequences are poorly conserved, allowing a consistent alignment only for the viruses from the three *Drosophila* species (Fig. S2). Only when we used an algorithm that takes secondary structures into consideration was it possible to align VP3 sequences from all Nora-like viruses (Fig. S3). At best, we see a modest extent of sequence conservation for amino acids 1–200, while the region downstream is very poorly conserved, barring a few amino acid positions. A sequence similarity with a consistency score of 5 or above was seen only at 19 amino acid positions, all of which fall within the α-helical region. Hence, secondary structure prediction is conserved, despite the modest sequence similarity, suggesting a vital function for the α-helical structural domain.

A closer inspection of the predicted coiled coil region shows further interesting features in VP3 of the *D. melanogaster* Nora virus. Unlike the Marcoil prediction (solid black line in Fig. 2A), the Paircoil algorithm predicts that the coiled coil is split into three separate segments, labeled CC1-3 in Fig. 2A, with a relatively low coiled coil probability for the middle segment (dashed line in Fig. 2). The repeat unit of a coiled coil is seven amino acids, or about two turns of the α-helix. Fig. 2B illustrates the color-coded probability for each amino acid in VP3 to be in any of these seven positions, labeled a-g. For the predicted coiled coil segment CC3 this generates a regular pattern where each 7-amino acid repeat is represented as a red diagonal. The phase of this pattern shifts by one position at the border between CC2 and CC3, suggesting a disruption of the coiled coil structure at this point. A second set of diagonals in CC1 and CC2, shifted by three positions from the major diagonals, indicates two possible orientations of these segments. In the *D. immigrans* Nora virus there are predicted phase shifts between CC1 and CC2, as well as between CC2 and CC3 (Fig. S1), suggesting discontinuities between all three segments. Finally, while no phase shifts are predicted in the corresponding coiled coil region of the Nora virus from *D. subobscura*, a helix-breaking proline residue at the border between CC2 and CC3 (black line in Fig. 2C) indicates that the regular α-helical conformation is interrupted in this place. We conclude that the most likely conformation for VP3 in all three *Drosophila* viruses include two or three separate coiled coil segments. Of these,

a Multicoil prediction suggests that CC1 is most likely engaged in coiled coil trimers, while the prediction for CC2 is more uncertain (green curves in Fig. 2 and Fig. S1). The prediction of a coiled coil trimer is consistent with our observation with GEMMA that VP3 has a tendency to form trimers (Fig. 1A). However, CC3 is predicted to form a dimer in the *D. immigrans* and *D. subobscura* viruses (purple curves) and there is no prediction of its higher order structure in the *D. melanogaster* Nora virus.

A sequence comparison between the three *Drosophila* Nora viruses (Fig. 2C, Fig. S2) shows that the CC1 segment is highly conserved; 76% of the positions are identical in all three species. CC2 is less well conserved (23% identical) and CC3 is even more variable (12% identical) and the latter segment has long indels at the N-terminus (Fig. S2). Outside the coiled coil domains, the N-terminal part is highly conserved (78%), but that region partially overlaps with the polymerase of ORF2 (grey region in Fig. 2C and Fig. S2) and it is uncertain how much of that sequence is included in the mature VP3. Finally, the C-terminal 1/3 of VP3, which is dominated by predicted β-strands and turns, is poorly conserved. Only 16% of the residues are identical in the three *Drosophila* viruses, most of them in the C-terminal 50 amino acids.

The CC1 segment is also well conserved in the Nora viruses from the tephritid flies, *B. latifrons*, *B. dorsalis* and *C. capitata*. A region of 68 residues, extending 20 residues upstream of CC1 and downstream into the border region to CC2, is 38–40% identical to the corresponding *D. melanogaster* sequence (Fig. 2C). Like *D. subobscura*, the tephritid viruses have a phase shift in the predicted coiled coil at the CC1-CC2 border (Fig. S1). Remaining parts of the tephritid viruses and the entire sequences of the lepidopteran and hymenopteran viruses are poorly conserved (Fig. S2) and they cannot be unambiguously aligned with the *Drosophila* virus sequences, but the predicted secondary structures are similar. All Nora viruses have a region with potential to form coiled coil trimers.

3.4. VP3 is critical for the fecal-oral transmission of Nora virus

In order to characterize the function of VP3 and the predicted coiled-coil motif, we constructed three mutants (Fig. 3A) using the cDNA clone of Nora virus. In the first mutant (NV-ΔVP3), three consecutive stop codons were introduced 97 nucleotides downstream of the 5′ end of ORF3, or 24 nucleotides downstream of the overlap with ORF2. The second mutant (NV-VP3ΔCC) is a deletion mutant, wherein 54 nucleotides corresponding to five turns of the α-helix, were deleted from ORF3, deleting parts of CC1 and CC2. In the third mutant (NV-truncVP3), three consecutive stop codons were introduced downstream of the posited coiled-coil. The generated clones were microinjected into fruit fly embryos to establish viral infection. Total RNA was extracted from injected animals and their offspring for quantitative RT-PCR analysis, in order to evaluate virus titers (Fig. 3B, note the logarithmic values). The wild-type cDNA clone of Nora virus (NV-Wt) was used as a control in all experiments. In previous experiments we injected fly embryos with Nora virus cDNA clones with non-replicating Nora virus genome sequences. After the injected embryos grew into adult we neither detected remains of the injected cDNA nor transcribed viral RNA. In contrast, we detected virus titers in all three virus mutants tested in this work, indicating that the genomes were replicating. The virus titer is reduced in the NV-ΔVP3 and NV-VP3ΔCC mutants, but it is near the wild-type level in NV-truncVP3. In addition, NV-Wt and the NV-truncVP3 mutants are also detected in the offspring of the injected animals. However, NV-ΔVP3 and NV-VP3ΔCC mutants are not detectable in the offspring, above the level where non-specific PCR products can be found (dashed line in Fig. 3B). This indicates that, although the NV-ΔVP3 and NV-VP3ΔCC mutants have replicating RNA genomes, they are not transmitted to the offspring. It is interesting to note that disruption of the coiled coil region leads to almost the same phenotype as removing the entire VP3 protein. Deleting the region downstream of the coiled coil appears to have a slight effect on the fitness of the virus, but not its replication or transmission, since the NV-truncVP3 mutant is present both in the injected animals and their offspring. This signifies that the coiled coil region is the imperative domain of VP3 and that it is essential for the transmission of Nora virus via the fecal-oral route. This opens up several possibilities, one of which is a role for this region in the assembly of virus particles.

We proceeded to examine whether these mutants were capable of assembling virions. To explore this possibility, we purified virus particles from whole fly extract and feces, collected from flies infected with NV-Wt, NV-ΔVP3, NV-VP3ΔCC or NV-truncVP3. Rate-zonal separation was used to purify the virus particles and quantitative RT-PCR was performed on total RNA isolated from the sucrose-gradient fractions (Fig. 3C). In this scenario, any signal obtained for the virus will have originated from assembled, intact virions. Also, unassembled capsid proteins will sediment very differently as compared to assembled virus particles. Hence, this method would give us an indication as to whether virions have been assembled for the different mutants. Assembled virus particles were detected in infected flies for all three mutants, signifying that mutation of VP3 did not affect the actual assembly of the virions. Particles were not detected in feces for the NV-ΔVP3 and NV-VP3ΔCC mutants in contrast to NV-Wt and NV-truncVP3 mutant particles, which were present in the feces also. This implied that, although virions are assembled for all the mutants, only the NV-truncVP3 particles can be detected in the feces. The fact that the NV-ΔVP3 and NV-VP3ΔCC particles are not detected in the feces explains why they are not horizontally transmitted to the offspring.

Taken together, these results indicate that the putative coiled-coil motif of VP3 is not involved in the replication of the viral genome or in the assembly of the virions. This domain is instead critical for the successful transport of the assembled particles to the feces or for the stability of the particles during or after transportation to the feces.

3.5. VP3-coiled coil domain aids transmission by stabilizing the virus particles

There are several proteases and enzymes within infected cells that can cause harm to virions. Additionally, since Nora virus replicates in the fruit fly midgut (Habayeb et al., 2009), it travels through the hostile environment of the fly gut, with varying pH conditions, digestive enzymes and proteases (Lemaitre and Miguel-Aliaga, 2013), before it reaches the feces. Upon arrival in the feces, the virions may once again face enzymes and proteases, secreted by defecated gut microbes, before successfully infecting a new host. We postulated that the conserved coiled-coil domain was crucial for the stability of the virions against adverse conditions within infected cells, either while they undertook the perilous passage through the fly gut, or upon defecation along with the feces.

First, we compared the stability of heated mutant particles to that of wild type particles. For this purpose, NV-Wt and mutant virions were purified from infected flies by rate-zonal separation and their content of viral RNA was quantified as shown in Fig. 3C. Only intact assembled virus particles will sediment at fractions close to the sedimentation rate of wild-type particles. Hence, RNA detected by quantitative RT-PCR would have originated from assembled virions or virion-like structures. The 2.5 ml and 3.0 ml sedimentation fractions were pooled and aliquoted into two equal volumes. One batch was subjected to heat treatment at 55 °C for 5 min, followed by RNase A treatment for 30 min at 37 °C. The second batch was subjected only to RNase A treatment. Total RNA was extracted from both sets of particles for each mutant and analyzed by quantitative RT-PCR. Any signal obtained would have originated from

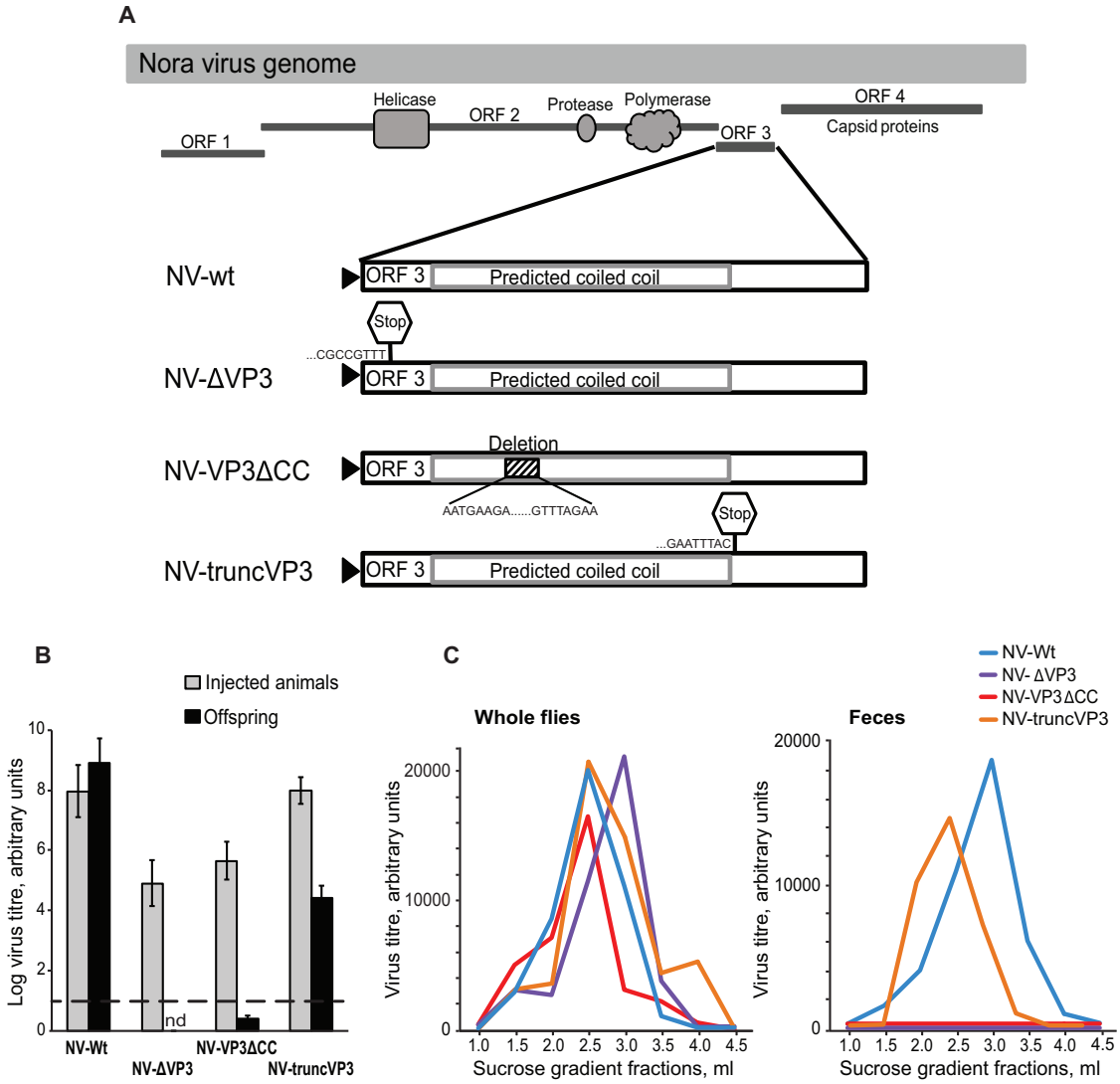

Fig. 3. VP3 is required for the transmission of Nora virus via the fecal-oral route. (A) Schematic representation of Nora virus VP3 mutants generated. (B) Nora virus was quantified by quantitative RT-PCR on total RNA from *Relish*^{E23} flies and their offspring, infected with either unmodified Nora virus (NV-Wt) or any one of the VP3 mutants (NV-ΔVP3, NV-VP3ΔCC and NV-truncVP3). The dotted line represents the point below which PCR artifacts appear, after 35 cycles of amplification. Such signals are also observed in negative controls without any template RNA. (C) Virus particles were purified from whole *Relish*^{E23} flies or from feces of such flies, infected with either NV-Wt or any one of the VP3 mutants, by rate-zonal separation on a sucrose gradient. Quantitative RT-PCR was performed on total RNA extracted from each collected fraction of the sucrose gradient. For (B) and (C), the results shown are an average of at least 3 independent experiments and error bars indicate standard deviation. Between 5–30 flies were used for each experiment, and the same number of flies were used for the control and the mutant being tested in that particular experiment.

intact virus particles, as free RNA released due to capsid disintegration would be degraded during RNase A treatment. This would hence give us an estimate of the particles that survived heat treatment without degradation. As shown in Fig. 4A, the NV-Wt and NV-truncVP3 particles resist heat treatment and can be detected at titers close to the unheated controls. On the other hand, the NV-ΔVP3 and NV-VP3ΔCC particles are almost entirely decimated (at least 1000-fold decrease) and can barely be detected after heat treatment. This clearly shows that the ability of Nora virus particles to withstand heat treatment is dependent on the coiled-coil motif but not the C-terminal third of the VP3 protein.

We next proceeded in a similar way to examine whether VP3 was important for the stability of the virions when treated with proteases. The combined 2.5 ml and 3.0 ml fractions of rate-zonally purified NV-Wt and mutant virus particles were divided into three equal volumes. The first set was treated with trypsin and the second set was treated with pancreatic protease, both followed by treatment with protease inhibitor cocktail and RNase A. The third set used as control was treated only with protease inhibitor and RNase A. Quantitative RT-PCR was performed on total RNA from the particles. Like in the heat-treatment experiment, the NV-Wt particles survived both trypsin and protease treatment without any significant loss of virions (Fig. 4B). The NV-truncVP3 virions appear to be only partially resistant to trypsin and protease treatment as a ten-fold loss of virions was observed. On the other hand, NV-ΔVP3 and NV-VP3ΔCC mutant particles were almost completely disintegrated as very little viral RNA was detected from these particles. This clearly signifies the importance of VP3 in the stability of the capsid structure under protease treatment. Based on the results from the heat-treatment experiment and the protease cleavage analysis, it is apparent that VP3 is critical for the stability of Nora virus virions. Specifically, the coiled-coil motif appears to be a functionally important domain involved in conferring stability to the capsid structure. The region downstream of the coiled-coil also

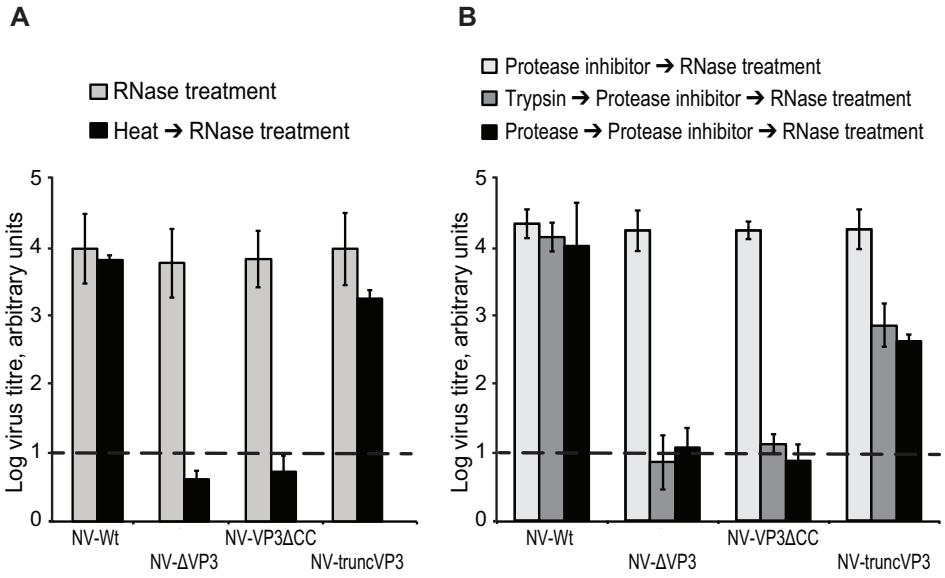

Fig. 4. VP3 is crucial for the stability of Nora virus Virions. (A) Purified virus particles were heat-treated at 55 °C for 5 min, followed by RNase A treatment. Control samples were treated only with RNase. qRT-PCR was performed on RNA from both heat-treated and unheated particles to estimate virus titer. This graph shows the loss of NV-ΔVP3 and NV-VP3ΔCC virions upon heat-treatment. (B) Purified virus particles were 1) treated with trypsin, followed by treatment with a protease inhibitor cocktail and RNase, 2) treated with protease, followed by treatment with a protease inhibitor cocktail and RNase, 3) treated with only the protease inhibitor cocktail and RNase. Quantitative RT-PCR was performed on RNA from all particles to calculate virus titer. This graph shows the severe disintegration of NV-ΔVP3 and NV-VP3ΔCC virions and a partial loss of NV-truncVP3 virions upon treatment with trypsin and protease. For (A) and (B), the results shown are an average of 3 experiments, wherein the error bars indicate standard deviation. Between 10–20 flies were used for each experiment, but the same number of flies were used for the control and the mutant being tested in that particular experiment. The dotted line represents the point below which all values are considered to be PCR artifacts since these are obtained from quantitative RT-PCR signals that appear after 35 cycles of amplification. Such signals are also observed in negative controls without any template RNA.

seems to have a moderate effect on the stability of capsid proteins, but it is apparently not crucial.

4. Discussion

Our results show that Nora virus VP3 is a primarily α-helical protein that forms trimers in its native conformation. The α-helical region is predicted to form a coiled-coil domain, split into three parts, and comparisons with sequences from other Nora viruses have shown that this arrangement is well conserved. To the best of our knowledge, no known structural proteins of the picorna-like viruses have been predicted or shown to have this motif. The appearance of VP3, along with VP4 proteins in virus particles (Ekström et al., 2011) suggested that it should be associated with the capsid proteins. It was shown that the structural proteins of Nora virus are distinctly different from that of known picorna-like viruses (Ekström et al., 2011), but the role of VP3 or its association with the capsid has not been studied before.

In *Picornaviridae*, each capsid protein, VP1, VP2, VP3 and VP4 (unrelated to the Nora virus proteins with similar names), has a role in the different stages of capsid assembly, maturation and stability (Arnold et al., 1987; Hellen and Wimmer, 1992a; Hellen and Wimmer, 1992b; Curry et al., 1997; Lin et al., 2009; Jiang et al., 2014). Hence, mutations in any of these proteins can adversely affect one or more stages of the virus life cycle. For example, mutations in the Poliovirus VP2 protein can disrupt the completion of morphogenesis and the eventual formation of mature viral particles (Compton et al., 1990). Further, single amino acid substitutions in the Foot and Mouth disease virus VP1 protein can render the virus acid-stable, while amino acid substitutions in the VP3 protein render the virus acid-labile (Caridi et al., 2015). Similar effects have been observed in other virus families such as the *Caliciviridae* and *Togaviridae* also. In the Norwalk virus, the VP2 protein associated with the shell domain of the viral capsid (Vongpunsawad et al., 2013) is known to be crucial for the expression and stability of the capsid proteins (Bertolotti-Ciarlet et al., 2003). An Alphavirus nucleocapsid protein contains a predicted α-helical coiled coil domain that is essential for the assembly of the nucleocapsid core (Perera et al., 2001). Similarly, the coiled coil domain of adenovirus protein pIX is stated to have an important role in self-association and trimer formation of pIX molecules (Rosa-Calatrava et al., 2001). The correct structural association of pIX is critical for the icosahedral capsid structure of adenoviruses (van Oostrum and Burnett, 1985; Furcinitti et al., 1989; Stewart et al., 1993). Thus, the role of certain capsid-associated proteins in the assembly, stability and maturation of virions have been proven in several viruses. Our work on Nora virus VP3 has revealed that this capsid-associated protein is indispensable for the stability of the virion structure. Disrupting the coiled-coil domain of Nora virus VP3 has serious implications on the stability of the virions, such that it affects the horizontal transmission of the virus. This further reinforces our premise that Nora virus VP3 is absolutely essential for the structural stability of the capsid proteins.

To understand the molecular mechanisms involved in capsid stability is important not only to gain knowledge of an elementary aspect of Nora virus biology, but also to characterize the host-pathogen relationship between a small RNA virus and its host. This relationship between Nora virus and the fruit fly also happens to be an excellent model to study novel pathways involved in immune responses against small RNA viruses. Understanding the biology of viruses also helps us understand better the different techniques they use to modify cellular behavior and to suppress anti-viral responses. It would indeed be very interesting to further dissect the mechanism behind how VP3 provides stability to the Nora virus virions.

Conflict of interests

The authors declare that there is no conflict of interests.

Acknowledgements

The purification of VP3 was planned and performed by the Umeå Protein Expertise Platform. We thank Jörgen Åden (Department of Chemistry, Umeå University) for helping us perform Circular Dichroism on VP3. This research was supported by grants from the Swedish Research Council, the Academy of Finland and the Sigrid Juselius Foundation.

Appendix A. Supplementary data

Supplementary data associated with this article can be found, in the online version, at http://dx.doi.org/10.1016/j.virusres.2016.06.011.

References

Anderson, N.G., Harris, W.W., Barber, A.A., Rankin Jr., C.T., Candler, E.L., 1966. Separation of subcellular components and viruses by combined rate- and isopycnic-zonal centrifugation. J. Natl. Cancer Inst. Monogr. 21, 253–283.
Arnold, E., Luo, M., Vriend, G., Rossmann, M.G., Palmenberg, A.C., Parks, G., Nicklin, M.J.H., Wimmer, E., 1987. Implications of the picornavirus capsid structure for polyprotein processing. Proc. Natl. Acad. Sci. 84, 21–25.
Baj, A., Colombo, M., Headley, J.L., McFarlane, J.R., Liethof, M.A., Toniolo, A., 2015. Post-poliomyelitis syndrome as a possible viral disease. Int. J. Infect. Dis. 35, 107–116.
Böhm, G., Muhr, R., Jaenicke, R., 1992. Quantitative analysis of protein far UV circular dichroism spectra by neural networks. Protein Eng. 5, 191–195.
Bertolotti-Ciarlet, A., Crawford, S.E., Hutson, A.M., Estes, M.K., 2003. The 3' end of Norwalk virus mRNA contains determinants that regulate the expression and stability of the viral capsid protein VP1: a novel function for the VP2 protein. J. Virol. 77, 11603–11615.
Caridi, F., Vázquez-Calvo, A., Sobrino, F., Martín-Acebes, M.A., 2015. The pH stability of foot-and-mouth disease virus particles is modulated by residues located at the pentameric interface and in the N terminus of VP1. J. Virol. 89, 5633–5642.
Compton, S.R., Nelsen, B., Kirkegaard, K., 1990. Temperature-sensitive poliovirus mutant fails to cleave VP0 and accumulates provirions. J. Virol. 64, 4067–4075.
Curry, S., Fry, E., Blakemore, W., Abu-Gazaleh, R., Jackson, T., King, A., Lea, S., Newman, J., Stuart, D., 1997. Dissecting the roles of VP0 cleavage and RNA packaging in picornavirus capsid stabilization: the structure of empty capsids of foot-and-mouth disease virus. J. Virol. 17, 9743–9752.
Delorenzi, M., Speed, T., 2002. An HMM model for coiled-coil domains and a comparison with PSSM-based predictions. Bioinformatics 18, 617–625.
Edwin, A., Grundström, C., Wai, S.N., Öhman, A., Stier, G., Sauer-Eriksson, A.E., 2014. Domain isolation, expression, purification and proteolytic activity of the metalloprotease PrtV from *Vibrio cholerae*. Protein Expr. Purif. 96, 39–47.
Ekström, J.O., Habayeb, M.S., Srivastava, V., Kieselbach, T., Wingsle, G., Hultmark, D., 2011. Drosophila Nora virus capsid proteins differ from those of other picorna-like viruses. Virus Res. 160, 51–58.
Fu, W., Lin, J., Cen, P., 2007. 5-Aminolevulinate production with recombinant *Escherichia coli* using a rare codon optimizer host strain. Appl. Microbiol. Biotechnol. 75, 777–782.
Furcinitti, P.S., van Oostrum, J., Burnett, R.M., 1989. Adenovirus polypeptide IX revealed as capsid cement by difference images from electron microscopy and crystallography. EMBO J. 8, 3563–3570.
Greenfield, N.J., 2006. Using circular dichroism spectra to estimate protein secondary structure. Nat. Protoc. 1, 2876–2890.
Habayeb, M.S., Ekengren, S.K., Hultmark, D., 2006. Nora virus, a persistent virus in *Drosophila*, defines a new picorna-like virus family. J. Gen. Virol. 87, 3045–3051.
Habayeb, M.S., Cantera, R., Casanova, G., Ekström, J.O., Albright, S., Hultmark, D., 2009. The *Drosophila* Nora virus is an enteric virus, transmitted via feces. J. Invertebr. Pathol. 101, 29–33.
Hedengren, M., Åsling, B., Dushay, M.S., Ando, I., Ekengren, S., Wihlborg, M., Hultmark, D., 1999. *Relish*, a central factor in the control of humoral but not cellular immunity in *Drosophila*. Mol. Cell 4, 827–837.
Hellen, C.U.T., Wimmer, E., 1992a. Maturation of poliovirus capsid proteins. Virology 187, 391–397.
Hellen, C.U.T., Wimmer, E., 1992b. The role of proteolytic processing in the morphogenesis of virus particles. Experientia 48, 201–215.
Jakubowska, A.K., D'Angiolo, M., González-Martínez, R.M., Millán-Leiva, A., Carballo, A., Murillo, R., Caballero, P., Herrero, S., 2014. Simultaneous occurrence of covert infections with small RNA viruses in the lepidopteran *Spodoptera exigua*. J. Invertebr. Pathol. 121, 56–63.
Jiang, P., Liu, Y., Ma, H.C., Paul, A.V., Wimmer, E., 2014. Picornavirus morphogenesis. Microbiol. Mol. Biol. Rev. 78, 418–437.
Koonin, E.V., Wolf, Y.I., Nagasaki, K., Dolja, V.V., 2008. The Big Bang of picorna-like virus evolution antedates the radiation of eukaryotic supergroups. Nat. Rev. Microbiol. 6, 925–939.
Laemmli, U.K., 1970. Cleavage of structural proteins during the assembly of the head of the bacteriophage T4. Nature 227, 680–685.
Lemaitre, B., Miguel-Aliaga, I., 2013. The digestive tract of *Drosophila melanogaster*. Annu. Rev. Genet. 47, 377–404.
Lin, J.Y., Chen, T.C., Weng, K.F., Chang, S.C., Chen, L.L., Shih, S.R., 2009. Viral and host proteins involved in picornavirus life cycle. J. Biomed. Sci. 16, 103.
McDonnell, A.V., Jiang, T., Keating, A.E., Berger, B., 2006. Paircoil2: improved prediction of coiled coils from sequence. Bioinformatics 22, 356–358.
Oliveira, D.C.S.G., Hunter, W.B., Ng, J., Desjardins, C.A., Dang, P.M., Werren, J.H., 2010. Data mining cDNAs reveals three new single stranded RNA viruses in *Nasonia* (Hymenoptera: Pteromalidae). Insect Mol. Biol. 19 (Suppl. 1), 99–107.
Perera, R., Owen, K.E., Tellinghuisen, T.L., Gorbalenya, A.E., Kuhn, R.J., 2001. Alphavirus nucleocapsid protein contains a putative coiled coil α-helix important for core assembly. J. Virol. 75, 1–10.
Petersen, B., Nordahl Petersen, T., Andersen, P., Nielsen, M., Lundegaard, C., 2009. A generic method for assignment of reliability scores applied to solvent accessibility predictions. BMC Struct. Biol. 9, 51.
Petersen, B., Lundegaard, C., Nordahl Petersen, T., 2010. NetTurnP – neural network prediction of beta-turns by use of evolutionary information and predicted protein sequence features. PLoS One 5, e15079.
Prisco, G.D., Zhang, X., Pennacchio, F., Caprio, E., Li, J., Evans, J.D., DeGrandi-Hoffman, G., Hamilton, M., Chen, Y.P., 2011. Dynamics of persistent and acute deformed wing virus infections in honey bees, *Apis mellifera*. Viruses 3, 2425–2441.
Pryor, K.D., Leiting, B., 1997. High-level expression of soluble protein in *Escherichia coli* using a His6-tag and maltose-binding-protein double-affinity fusion system. Protein Expr. Purif. 10, 309–319.
Rofougaran, R., Crona, M., Vodnala, M., Sjöberg, B.M., Hofer, A., 2008. Oligomerization status directs overall activity regulation of the *Escherichia coli* class Ia ribonucleotide reductase. J. Biol. Chem. 283, 35310–35318.
Rosa-Calatrava, M., Grave, L., Puvion-Dutilleul, F., Chatton, B., Kedinger, C., 2001. Functional analysis of adenovirus protein IX identifies domains involved in capsid stability, transcriptional activity, and nuclear reorganization. J. Virol. 75, 7131–7141.
Spradling, A.C., 1986. P element-mediated transformation. In: Roberts, D.B. (Ed.), Drosophila: A Practical Approach. IRL Press, Oxford, pp. 175–197.
Stewart, P.L., Fuller, S.D., Burnett, R.M., 1993. Difference imaging of adenovirus: bridging the resolution gap between X-ray crystallography and electron microscopy. EMBO J. 12, 2589–2599.
van Mierlo, J.T., Bronkhorst, A.W., Overheul, G.J., Sadanandan, S.A., Ekström, J.-O., Heestermans, M., Hultmark, D., Antoniewski, C., van Rij, R.P., 2012. Convergent evolution of argonaute-2 slicer antagonism in two distinct insect RNA viruses. PLoS Pathog. 8, e1002872.
van Mierlo, J.T., Overheul, G.J., Obadia, B., van Cleef, K.W.R., Webster, C.L., Saleh, M.-C., Obbard, D.J., van Rij, R.P., 2014. Novel Drosophila viruses encode host-specific suppressors of RNAi. PLoS Pathog. 10, e1004256.
van Oostrum, J., Burnett, R.M., 1985. Molecular composition of the adenovirus type 2 virion. J. Virol. 56, 439–448.
Vongpunsawad, S., Venkataram Prasad, B.V., Estes, M.K., 2013. Norwalk virus minor capsid protein VP2 associates within the VP1 shell domain. J. Virol. 87, 4818–4825.
Wolf, E., Kim, P.S., Berger, B., 1997. MultiCoil: a program for predicting two- and three-stranded coiled coils. Protein Sci. 6, 1179–1189.
Yang, H., Kronhamn, J., Ekström, J.O., Korkut, G.G., Hultmark, D., 2015. JAK/STAT signaling in *Drosophila* muscles controls the cellular immune response against parasitoid infection. EMBO Rep. 16, 1664–1672.